MICROBIAL ECOLOGY

Microb Ecol (2003) 46:371–390
DOI: 10.1007/s00248-002-0108-2

Microbial Mats on the Orkney Islands Revisited: Microenvironment and Microbial Community Composition

A. Wieland,[1] M. Kühl,[1] L. McGowan,[2] A. Fourçans,[3] R. Duran,[3] P. Caumette,[3] T. García de Oteyza,[4] J.O. Grimalt,[4] A. Solé,[5] E. Diestra,[5] I. Esteve,[5] R.A. Herbert[2]

[1] Marine Biological Laboratory, University of Copenhagen, Strandpromenaden 5, DK-3000 Helsingør, Denmark
[2] Division of Environmental and Applied Biology, School of Life Sciences, University of Dundee, Dundee DD1 4HN, UK
[3] Laboratoire d'Ecologie Moléculaire-Microbiologie, Université de Pau et des Pays de l'Adour, Avenue de l'Université, IBEAS, F-64000 Pau, France
[4] Department of Environmental Chemistry (ICER-CSIC), Jordi Girona 18, E-08034 Barcelona, Spain
[5] Department of Genetics and Microbiology, Autonomous University of Barcelona, E-08193 Bellaterra, Spain

Received: 7 November 2002; Accepted: 4 March 2003; Online publication: 14 August 2003

Abstract

The microenvironment and community composition of microbial mats developing on beaches in Scapa Flow (Orkney Islands) were investigated. Analysis of characteristic biomarkers (major fatty acids, hydrocarbons, alcohols, and alkenones) revealed the presence of different groups of bacteria and microalgae in mats from Waulkmill and Swanbister beach, including diatoms, Haptophyceae, cyanobacteria, and sulfate-reducing bacteria. These analyses also indicated the presence of methanogens, especially in Swanbister beach mats, and therefore a possible role of methanogenesis for the carbon cycle of these sediments. High amounts of algal lipids and slightly higher numbers (genera, abundances) of cyanobacteria were found in Waulkmill Bay mats. However, overall only a few genera and low numbers of unicellular and filamentous cyanobacteria were present in mats from Waulkmill and Swanbister beach, as deduced from CLSM (confocal laser scanning microscopy) analysis. Spectral scalar irradiance measurements with fiber-optic microprobes indicated a pronounced heterogeneity concerning zonation and density of mainly anoxygenic phototrophs in Swanbister Bay mats. By microsensor and T-RFLP (terminal restriction fragment length polymorphism) analysis in Swanbister beach mats, the depth distribution of different populations of purple and sulfate-reducing bacteria could be related to the microenvironmental conditions. Oxygen, but also sulfide and other (inorganic and organic) sulfur compounds, seems to play an important role in the stratification and diversity of these two major bacterial groups involved in sulfur cycling in Swanbister beach mats.

Correspondence to: A. Wieland; E-mail: awieland@zi.ku.dk

Introduction

Laminated microbial communities frequently develop in the upper intertidal zone of sandy beaches and tidal flats (e.g., [79, 16, 87, 49]). After initial colonization and succession of cyanobacteria [79], the mature states of these stratified phototrophic communities develop into microbial mats, consisting of a thin top layer of sand and/or diatoms covering a dense layer of filamentous cyanobacteria. Below the cyanobacteria, a distinct layer of purple sulfur bacteria is often present with a reduced black layer of precipitated iron sulfides underneath due to intensive sulfate reduction [84]. Sulfate-reducing bacteria are also present at high numbers in the upper millimeters of the mats [88, 98]. Because of the macroscopically visible lamination such coastal microbial mats were named colored sands or "Farbstreifensandwatt" [33]. Both cyanobacteria and anoxygenic phototrophs contribute to sediment binding and stabilization of the sediment [28]. The dominant cyanobacterium is generally *Microcoleus chthonoplastes* [79, 16, 84, 89], whereas the immotile *Thiocapsa roseopersicina* is often the dominant purple sulfur bacterium [16, 87, 84].

Mass blooms of purple sulfur bacteria, mainly *T. roseopersicina*, have been observed during summer in the intertidal zone of sheltered sandy beaches in Scapa Flow on the Orkney Islands [31, 85, 86]. Three different laminated microbial mats were described [86], distinguished by the position of the cyanobacterial layer above or beneath the purple sulfur bacterial layer, or by its complete absence and therefore exclusive development of purple sulfur bacteria in the top layer of the sediment. Mats with a typical lamination pattern (see above) were most common [86]. However, cyanobacteria were only present at relatively low population densities, and *M. chthonoplastes* was absent in all investigated mats [86].

The beaches of Scapa Flow are locally enriched in nitrogen-containing organic matter due to decomposition of accumulated macroalgal debris [31, 86]. In Scapa Bay, additional organic matter was supplied by discharges from local whiskey distilleries [86]. The high organic carbon content of the sediments leads to availability of low molecular weight organic substrates for sulfate-reducing bacteria, and the produced sulfide serves as an electron donor for anoxygenic photosynthesis by purple sulfur bacteria [31]. Distinct microcolonies formed by the purple sulfur bacteria (mainly *T. roseopersicina*) can effectively bind sediment grains. This aggregation leads to a reduction of erosion and, therefore, to a stabilization of the sediment [85]. Although these aggregates may not be as effective as the cohesive structures of cyanobacterial mats in stabilizing sandy sediments and preventing erosion, purple sulfur bacteria and mainly *T. roseopersicina* were capable of rapidly recolonizing eroded sites on beaches in Scapa Flow [85].

Further characteristics of these sediment ecosystems dominated by purple sulfur bacteria are the absence of chemolithotrophic sulfur bacteria, normally present in marine microbial mats [88], and the almost permanent exposure of purple sulfur bacteria to O_2 at the sediment surface [85, 86].

In this study, the composition of the microbial community and the microenvironmental conditions in microbial mats from Orkney Islands beaches was investigated. This included determination of phototrophic populations with confocal laser scanning microscopy (CLSM) and fiber-optic microprobe-based spectrometry in microbial mats from Waulkmill and Swanbister beaches. Dominant groups of mat-inhabiting microorganisms were determined by their characteristic biomarkers. Furthermore, the stratification of major bacterial groups in relation to microenvironmental gradients was investigated in Swanbister beach mats. For this, O_2 and sulfur cycling was quantified by controlled microsensor experiments in the laboratory and by sulfate reduction rate measurements. The depth-zonation and diversity of the entire microbial community and of the major bacterial groups involved in sulfur cycling in Swanbister beach mats were analyzed with terminal restriction fragment length polymorphism (T-RFLP).

Materials and Methods

Sampling

Sediment samples were taken in July 2000 at low tide with Plexiglas core tubes (53 mm i.d.) on beaches of Waulkmill and Swanbister Bay located in Scapa Flow, Orkney Islands (a map with locations can be found in [86]). *In situ* temperature and salinity of remaining stagnant seawater were 12–13°C and 40‰ at the time of sampling. Downwelling irradiance around noon on clear and sunny days was >1100 μmol photons $m^{-2}s^{-1}$. Sampled sediment cores were transported to the laboratory of the Orkney County Council Marine Unit on Orkney Island (Mainland), where microsensor measurements were performed under controlled conditions.

Microsensor Measurements

Clark-type O_2 [72] and H_2S [36, 50] microsensors connected to a picoammeter (Unisense A/S, Denmark), and glass pH microelectrodes [74] connected to a high-impedance mV-meter (WPI Inc., USA) were used for fine-scale measurements of O_2 and sulfide distribution in Swanbister beach mats. Oxygenic gross photosynthesis was quantified with the light–dark shift method [73]. The O_2 microsensor had a tip diameter of 10 μm, a stirring sensitivity of ~1%, and a response time, t_{90}, of ~0.4 s. The H_2S microsensor had a tip diameter of 40 μm and was coated with a black enamel paint to avoid light interference [50]. The length and the tip diameter of the pH-sensitive glass of the pH microelectrode were 250 and 10 μm, respectively.

The O_2 microsensor was linearly calibrated in the experimental setup (see below) by a two-point calibration using readings of microsensor current in the air saturated overlying water (100% air saturation) and in the anoxic part of the mats (0% O_2). Dissolved O_2 concentrations of air saturated seawater at experimental temperatures and salinities were calculated according to García and Gordon [27]. The pH microelectrode was calibrated in standard buffer solutions (Radiometer, Denmark). The pH of the overlying water in the experimental setup was determined with a commercial pH meter calibrated in standard buffer solutions (Radiometer, Denmark). The readings of the pH microelectrode in the overlying water were adjusted to the measured pH of the seawater. The H_2S microsensor was calibrated in anoxic buffer solutions (0.2 M phosphate buffer, pH 7.5) of increasing sulfide concentrations. A sample of each sulfide buffer solution was fixed in zinc acetate (5% w/v) for subsequent spectrophotometric analysis of sulfide concentration after Fonselius [23] with modifications, i.e., acidification of the samples to pH <1 with 6 M HCl and determination of the absorption of the formed complex at the second peak (750 nm) in the spectrum (C. Steuckart, unpublished). Calculation of H_2S and total sulfide (S_{tot}) concentration profiles from H_2S and pH microsensor data was as described in Wieland and Kühl [97], using pK_1 values calculated from experimental temperatures according to Hershey et al. [32].

Experimental Microsensor Setup

Sediment cores were mounted in a flow chamber modified for insertion of whole sediment cores [21]. A constant flow over the mat surface of aerated seawater from the sampling site was generated with a submersible water pump (Aqua Clear, Germany) connected to the flow chamber. Measurements were performed at room temperature (21°C ± 1°C). The mat was illuminated with a fiber-optic halogen light source (KL 2500, Schott, Germany) and the downwelling irradiance at the mat surface was quantified with an underwater quantum irradiance meter (QSL-101, Biospherical Instruments, USA). The microsensors were fixed together with the measuring tips in the same horizontal plane within an area of ca. 0.5–1 cm^2 of the mat surface in a motor-driven micromanipulator (Märzhäuser, Germany; Oriel, USA) mounted on a heavy solid stand. Microsensor signals were recorded with strip chart recorders (Servogor, UK; Kipp & Zonen, The Netherlands) and with a computer data acquisition system (LabView, National Instruments, USA) that also controlled the micromanipulator. Gross photosynthesis measurements in steps of 100- or 200-μm vertical depth intervals were performed as described in Wieland and Kühl [97].

Spectral Scalar Irradiance Measurements with Fiber-Optic Microprobes

A fiber-optic scalar irradiance microprobe [52] was connected to a sensitive fiber-optic diode array spectrometer with a spectral range of 250–950 nm (PMA-11, Hamamatsu Photonics, Japan). Profiles of spectral scalar irradiance in the mats were measured by stepwise inserting the microprobe with a motor-driven micromanipulator (Märzhäuser, Germany; MICOS GmbH, Germany; Jenny Electronics AG, Switzerland) at a zenith angle of 135° relative to the incident light beam. The mats were illuminated vertically with a fiber-optic halogen light source (KL 2500, Schott, Germany). Measurements were performed at vertical depth intervals of 200 μm. The downwelling spectral scalar irradiance at the mat surface was measured by positioning the scalar irradiance microprobe over a black light trap at the same position relative to the light field as the mat surface. Scalar irradiance spectra at various depths in the mats were normalized to the downwelling scalar irradiance at the mat surface. Attenuation spectra of scalar irradiance were calculated over discrete depth intervals from the depth profiles of spectral scalar irradiance by

$$K_0 = \ln(E_1/E_2)/(z_2 - z_1) \quad (1)$$

where K_0 is the vertical spectral attenuation coefficient for scalar irradiance, and E_1 and E_2 are the spectral scalar irradiance measured at depths z_1 and z_2 in the mat, where $z_2 > z_1$ [48].

Calculations

Diffusive O_2 fluxes across the mat-water interface were calculated from O_2 profiles using Fick's first law of diffusion as described in Wieland and Kühl [96]. Areal rates of O_2 consumption in the aphotic zone, R_{aphot}, were calculated as the downward O_2 flux, J_s, at the lower boundary of the photic zone:

$$J_s = -\phi D_s \, dC/dz \quad (2)$$

where dC/dz is the linear concentration gradient, ϕ is the sediment porosity, and D_s is the sediment diffusion coefficient, which was calculated from the porosity and D_0 according to Ullman and Aller [83]. The D_0 of O_2 was taken from Broecker and Peng [8] and corrected for experimental temperatures and salinities [53]. Fluxes of H_2S were calculated according to Eq. 2 from the linear part of the profiles. The diffusion coefficient of H_2S was estimated as $D_0(H_2S)=0.7573\ D_0(O_2)$ (Tables for seawater and gases, Unisense A/S, Denmark).

Determination of Sediment Porosity

Sediment porosity (mL water cm^{-3}) was determined ($n = 5$) on samples collected from Swanbister Bay in July 2001 using a 2.5-cm diameter stainless steel corer. The cores were sectioned using a sediment slicer to give the following four consecutive depth horizons: 0–5 mm, 5–10 mm, 10–20 mm, and 20–30 mm. Porosity was measured as weight loss after drying at 110°C for 24 h.

Determination of Sulfate Reduction Rates

Triplicate sediment cores (13 mm i.d.) were collected from Swanbister Bay in truncated 5-mL disposable syringes and sealed with Suba seals (W. Freeman Ltd., UK). Carrier-free $^{35}SO_4^{2-}$ (10 μL; Amersham Pharmacia Biotech, UK) was injected through the Suba seal using a microliter syringe into each sediment core, giving an average activity of 50 kBq cm^{-3}. To ensure even distribution of the isotope throughout the cores the isotope was added progressively as the syringe needle was withdrawn. At the end of the 12-h incubation period at ambient temperature (16°C) in the dark, the cores were sectioned to give the following depth horizons: 0–10 mm, 10–20 mm, and 20–30 mm. Each sediment section was transferred to plastic bottles containing 5 mL of a 20% w/v zinc acetate solution to stop biological activity and preserve sulfide. The samples were then frozen and stored until they were required for analysis. Production of $H_2^{35}S$ was determined using the one-step distillation method of Fossing and Jørgensen [24]. Sulfate reduction rates were calculated according to the method of Isaksen and Finster [35]. Porewater sulfate was determined according to the method of Tabatabai [80].

Confocal Laser Scanning Microscopy

Sediment cores (18 mm i.d.) were taken from Waulkmill and Swanbister Bay using truncated 20-mL disposable syringes. The samples were transferred into small plastic containers containing 2.5% glutaraldehyde in a phosphate buffer (0.2 M) adjusted to the appropriate salinity with NaCl. The samples were fixed for 3 h and then washed 2–3 times with phosphate buffer. The samples were stored at 4°C until further analysis.

The samples were investigated with a compound microscope (Olympus BH2, Japan) and a laser confocal microscope (Leica TCS 4d, Germany) equipped with an argon–krypton laser. For confocal analysis, subsamples (slices) of defined dimension were placed in cavity slides, covered and sealed with coverslips, and observed under an excitation beam of 568 nm. Pigment fluorescence emission was detected with a 590 nm long-pass filter. Optical sections (every focal plane), optical series (all focal planes from each imaged area), summa images (all optical series projected to one image), and stereoscopic images (one image in three dimensions from every optical series) were obtained from these analyses. A volume data set was generated by combining all optical sections.

After screening of the different cyanobacteria present in all images from each sampling site, each type of cyanobacterium was identified after morphological criteria according to Castenholz [10].

Analysis of Fatty Acids, Hydrocarbons, Alcohols, and Alkenones

Sediment cores (26 mm i.d.) were collected on Waulkmill and Swanbister beach and stored frozen until further analysis. The upper 4 cm of the mat samples (approximately 10 g) were homogenized with a mortar and extracted three times with methanol, dichloromethane, and *n*-hexane. Extracts were saponified with 30 mL of KOH (6% w/v) in methanol and the neutral components were recovered by extraction with 3 × 30 mL of *n*-hexane. The alkaline mixture was then acidified to pH 2 with 5 mL of HCl, and the acidic compounds were recovered by extraction with 3 × 30 mL of *n*-hexane. The neutral compounds were fractionated in a column filled with silica (8 g, bottom) and alumina (8 g, top). These packings were prepared previously by heating at 120°C and 350°C for 12 h, respectively. Milli-Q water was added to both adsorbents for deactivation (5%). Six fractions were obtained by successive elution with 20 mL of *n*-hexane, 20 mL of *n*-hexane/dichloromethane (9:1), 40 mL of *n*-hexane/dichloromethane (8:2), 40 mL of *n*-hexane/dichloromethane 75% (1:3), 20 mL of dichloromethane/methanol (95:5), and 40 mL of dichloromethane/methanol (9:1). The two most polar fractions were silylated after redissolution in 100 μL of dichloromethane and addition of 100 μL bis(trimethylsilyl)trifluoroacetamide (heating 1 h at 60°C). The fatty acid fractions were methylated before instrumental analysis using diazomethane, which was synthesized as described elsewhere [91]. These fractions were dissolved in 100 μL of *n*-hexane and diazomethane was added until the yellowish color remained.

Samples were analyzed by gas chromatography and flame ionization detection in a Varian Star 3400 (Varian Inc., USA). A 30 m capillary column (0.25 mm i.d.) coated with DB-5 (25 μm film thickness) was used with hydrogen as carrier gas. The oven was kept at 70°C for 1 min, heated to 140°C at 10°C/min, then to 310°C at 4°C/min, and finally held at 310°C for 30 min. The temperature of the detector was 330°C. Analyses by gas chromatography and mass spectrometric detection were performed with a Fisons MD-800 quadrupole mass analyzer (Thermo Instruments, UK). Samples were injected in splitless mode at 300°C into a 30 m capillary column (0.25 mm i.d.) coated with DB-5 (25 μm film thickness). Helium was used as carrier gas and the temperature program was as described above. Mass spectra were recorded in electron impact mode at 70 eV by scanning between m/z 50–650 every second. Ion source and transfer line were kept at 300°C.

T-RFLP Analysis

Sediment cores (35 mm i.d.) were taken with Falcon tubes from Swanbister Bay. The upper 10 mm of the sediment core was sliced off aseptically, transferred to sterile petri dishes, frozen in liquid nitrogen, transported on dry ice, and finally stored at −80°C until further analysis. The upper 2 mm of the mat cores

Table 1. Phylogenetic and photosynthetic primers used in T-RFLP analysis[a]

Primer	Sequence (5′ → 3′)	Target gene	Target group	Reference
8F	AGA GTT TGA TCC TGG CTC AG	*ssu 16S rDNA*	Eubacteria	[54]
926R	CCG TTC AAT TCC TTT RAG TTT	*ssu 16S rDNA*	Eubacteria	[54]
BSR 385R	CGG CGT CGC TGC GTC AGG	*ssu 16S rDNA*	SRB	[2]
PB 557F	CGCACCTGGACTGGAC	*PufM*	PAB	[1]
PB 750R	CCCATGGTCCAGCGCCAGAA	*PufM*	PAB	[1]

[a] Amplimer sizes for the different primer sets: *16S rDNA* eubacteria, 918 bp; *16S rDNA* sulfate-reducing bacteria, 377 bp; *pufM*, 229 bp. All 16S rDNA primer names are based on *E. coli* numbering. SRB denotes sulfate-reducing bacteria and PAB purple anoxygenic bacteria

was sliced with a cryomicrotome (MICROM GmbH, Germany) at around 200 μm, and the third millimeter at around 500 μm vertical depth resolution. From these mat slices, DNA was extracted with the UltraClean Soil DNA Isolation Kit using the alternative lysis method (MoBio Laboratories Inc., USA). All extracted genomic DNA samples were stored at −20°C until further processing.

The different primers used for T-RFLP analysis to assess the bacterial community structure are listed in Table 1. For T-RFLP analysis, forward (f) and reverse (r) primers were fluorescently labeled with TET and HEX (E.S.G.S. Cybergene group, France), respectively. The PCR amplification mixture contained 12.5 μL hot start *Taq* polymerase mix (Qiagen, Netherlands), 0.5 μL of each primer (20 μM), and 1 μL of DNA template. A final volume of 50 μL was adjusted with distilled water. Reactions were cycled in a PTC200 thermocycler (MJ Research, USA) at 94°C for 15 min, followed by 35 cycles of 94°C for 1 min; T_m for 1.5 min, with T_m denoting the corresponding melting temperature for hybridization between primers and template DNA; and 72°C for 1 min, with a final extension step at 72°C for 10 min. The amount of PCR product was determined by comparison to known concentrations of standards (Smartlader, Eurogentec, Belgium). PCR products were purified with the GFX PCR DNA purification kit (Amersham, UK).

Purified PCR products (600 to 700 ng) were digested with 12 units of enzyme *Hae*III or *Hin*6I (New England Biolabs, USA). The precise length of T-RFs from the digested PCR products was determined by capillary electrophoresis (ABI prism 310, Applied Biosystems, USA). About 50 ng of the digested DNA from each sample was mixed with 10 μL of deionized formamide and 0.25 μL of TAMRA size standard and then denatured at 94°C for 2 min and immediately chilled on ice prior to electrophoresis. After an injection step of 10 s, electrophoresis was carried out for up to 30 min applying a voltage of 15 kV. T-RFLP profiles were performed using GeneScan software (ABI).

Dominant T-RFs were selected by comparison of numerical values and electropherograms. The clustering values were analyzed with the T-RFLP similarity matrix on the RDP (Ribosomal Database Project) Web site (http://rdp.cme.msu.edu/) [56]. The obtained distance matrix was used to construct a dendrogram with MEGA version 2.1 [51] using the UPGMA method (Unweighted Pair Group Method with Arithmetic Mean).

T-RFLP profiles were also compared by Canonical Correspondence Analysis (CCA) according to Fromin et al. [25]. This test is based on the linear correlation between community data (abundance of each T-RF) and environmental parameters in the mat at light conditions (scalar irradiance at wavelengths of Chl *a* [676 nm] and BChl*a* [845 nm] absorption, depth, and O_2 concentration). The CCA were realized with MVSP v3.13d software (Rockware Inc., UK).

Results

Biomarkers in Waulkmill and Swanbister Bay Mats

The major lipid compounds in both Waulkmill and Swanbister beach mats were fatty acids, encompassing essentially C_{14}–C_{22} homologues dominated by *n*-hexadec-9(*Z*)-enoic and *n*-hexadecanoic acids (Fig. 1A, B). Other major compounds were *n*-octadec-9(*Z*)-enoic, *n*-eicosapentenoic, *n*-tetradecanoic, and *n*-pentadecanoic acids, which are generally representative of algal and microbial contributions. *N*-Octadec-9(*Z*)-enoic acid is abundant in photosynthetic algae and cyanobacteria [11]. *N*-Eicosapentenoic acid and other polyunsaturated *n*-eicosane and *n*-docosane acids are specific of inputs from diatom species [93]. *Iso*- and *anteiso*-pentadecanoic acids were the two main branched fatty acids present in significant proportions. These compounds are abundant in sulfate-reducing bacteria and sulfur-oxidizing bacteria such as *Thiomicrospira* [29].

The aliphatic hydrocarbon phyt-1-ene together with other phytene homologues occurred in both mats, but their presence was more pronounced in the Swanbister mat (Fig. 1C, D). These hydrocarbons are characteristic for methanogens [82] and may also be produced during the decomposition of phytol [18]. The presence of an isoprenoid compound specific of methanogenic origin, 2,6,10,15,19-pentamethylicosane [34, 75], in the Swanbister mat (Fig. 1C) suggests that at least in this mat the occurrence of the phytanes is due to inputs from these microorganisms. *N*-Heptadecane and *n*-heptadecenes were major compounds in both mats and especially abundant in the Waulkmill mat (Fig. 1D). These compounds are

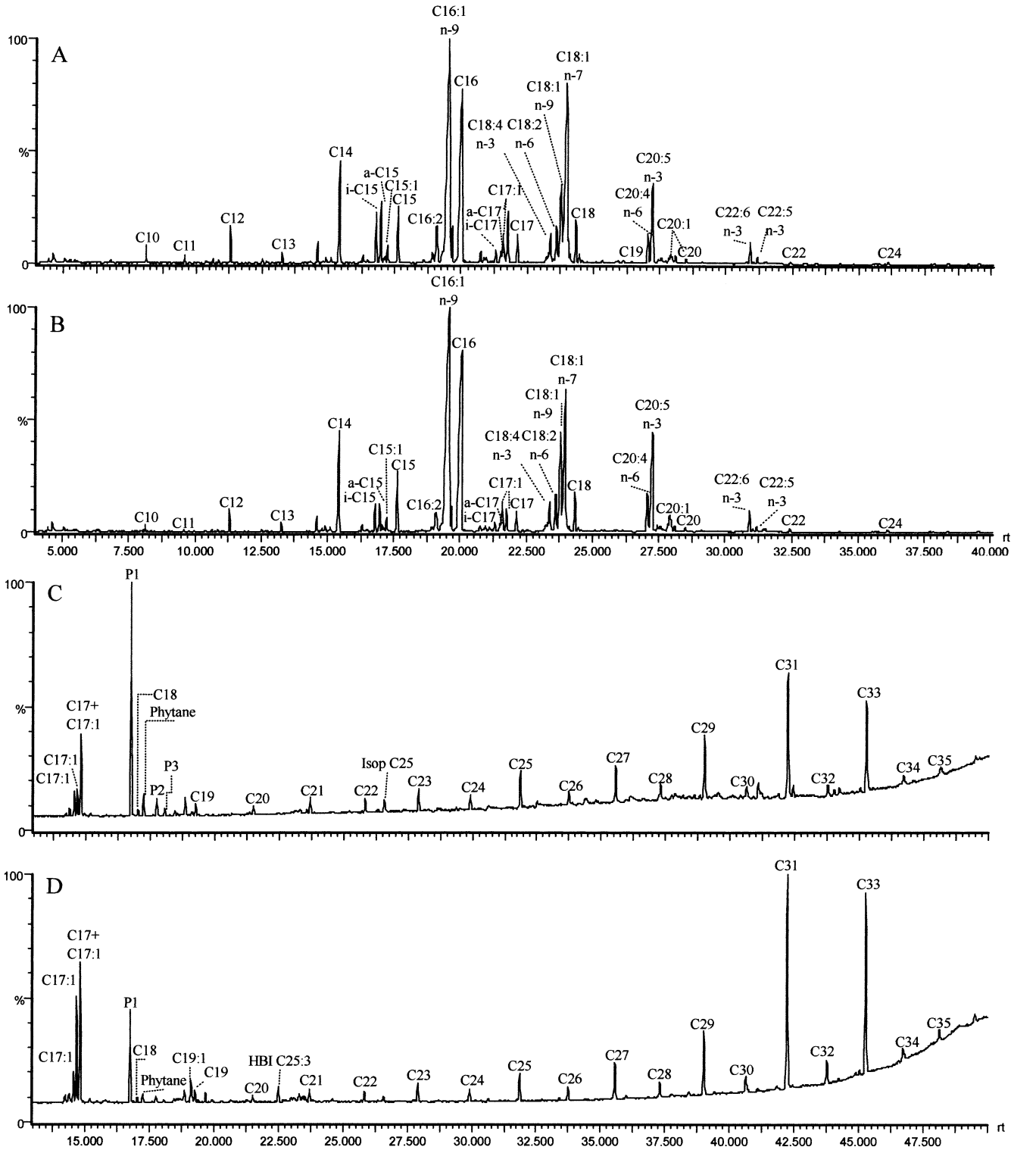

Fig. 1. Gas chromatographic profiles showing the major fatty acids (A, B) and the major hydrocarbons (C, D) in microbial mats from Swanbister (A, C) and Waulkmill (B, D) Bay. P1 denotes phyt-1-ene and P2 and P3 are phytenes. HBI C25, highly branched isoprenoid hydrocarbon. Isop C_{25}, 2,6,10,15,19-pentamethylicosane.

generally found in cyanobacteria [30, 67] or in phototrophic eukaryotes [7]. Other hydrocarbons specific for algal inputs such as C_{25} highly branched isoprenoid alkenes synthesized by diatoms [62] were also present in the

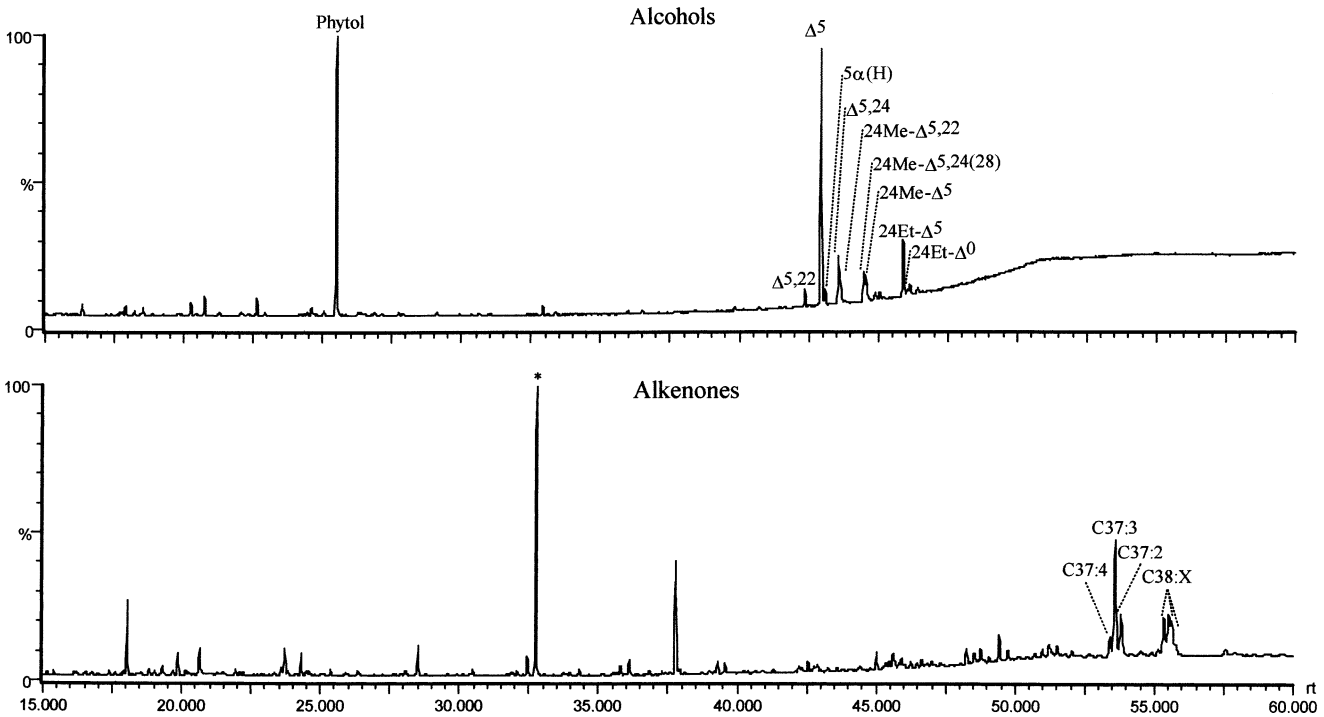

Fig. 2. Gas chromatographic profiles showing the major alcohols (upper graph) and alkenones (lower graph) in Waulkmill Bay mats.

Waulkmill mat. In addition to these hydrocarbons, a distribution of C_{23}–C_{35} *n*-alkanes predominated by the odd carbon numbered homologues, namely C_{29}, C_{31}, and C_{33}, representative for inputs from higher plants [20], were found in both mats. This distribution can also be found in other sediments in coastal environments [5], probably reflecting the influence of wind-transported materials from nearby higher plants.

A significant amount of phytol was found in the Waulkmill mat, representing contributions from algae (Fig. 2). Other lipids of algal origin, such as C_{37}–C_{38} di-, tri-, and tetraunsaturated alkenones specific for Haptophyceae [92, 57] and sterols, were also present. The sterol distribution in the Waulkmill mat was dominated by cholest-5-en-3β-ol and contains minor proportions of 24-ethylcholest-5-en-3β-ol, cholesta-5,24-dien-3β-ol, 24-methylcholesta-5,24(28)-dien-3-ol, and their homologues saturated at Δ^5 (Fig. 2, upper graph). Sterols unsaturated at positions Δ^5, Δ^{22}, and $\Delta^{5,22}$ can originate from cyanobacteria [67, 61, 63], green algae [68, 4] or diatoms [64, 41, 4]. 24-Methylcholesta-5,24(28)-dien-3β-ol is a common diatom marker [64, 41, 4], and its occurrence is consistent with the presence of highly branched isoprenoid hydrocarbons.

Spectral Scalar Irradiance and Cyanobacteria in Waulkmill Bay mats

From spectral scalar irradiance profiles the zonation of phototrophs in the mats could be inferred from the absorption characteristics of their pigments at specific wavelengths. In the Waulkmill mat, three main wavelength regions of pronounced absorption could be identified (Fig. 3). The pronounced minimum of scalar irradiance in the narrow region around 675 nm corresponds to Chl *a* absorption, indicating the presence of cyanobacteria and/or microalgae. A shoulder in the spectra measured over the upper 2 mm indicated some absorption at ~625 nm due to the presence of phycocyanin. The presence of purple bacteria throughout the upper millimeters of the mat was indicated by the pronounced minima in the region from 760 to 900 nm and at around 590 nm corresponding to BChl *a* absorption. The scalar irradiance in these wavelength regions was already at 1 mm depth less than 50% of the downwelling scalar irradiance at the mat surface and at 2.6 mm depth less than 1–2%. The strong absorption by Chl *a* and BChl *a* indicates the presence of dense populations of oxygenic and anoxygenic phototrophs in the upper 2.6 mm of the mat.

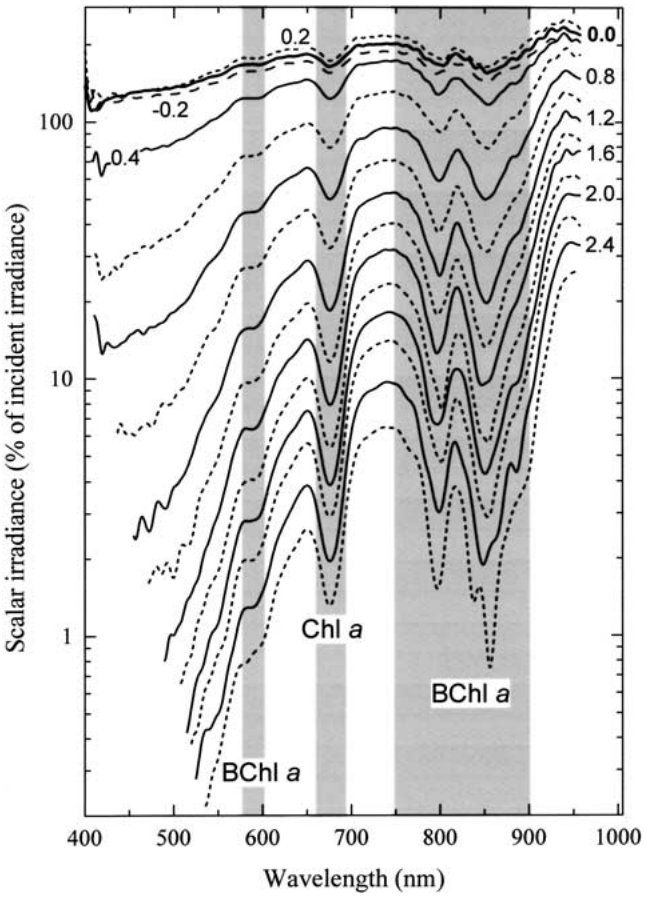

Fig. 3. Depth profile of spectral scalar irradiance in a Waulkmill Bay mat normalized to the downwelling spectral scalar irradiance at the mat surface. Numbers on curves indicate depth (mm). Depth 0 indicates the mat surface and increasing positive numbers indicate increasing depths in the mat.

Several different genera of filamentous and unicellular cyanobacteria were identified (Table 2), with cyanobacteria of the genera *Lyngbya* and *Oscillatoria* and of the *Pleurocapsa* and *Gloeocapsa* groups being the most abundant in the Waulkmill Bay mat as observed with CLSM and light microscopy. Some cyanobacteria occurred only at certain depths of the mat, whereas others were found in several or all mat slices investigated.

Spectral Scalar Irradiance and Cyanobacteria in Swanbister Bay Mats

In a Swanbister Bay mat, spectral scalar irradiance minima at characteristic Chl *a* and BChl *a* absorption wavelengths were found (Fig. 4). Pronounced light scattering was detected at the mat surface and in the uppermost mat layers. Wavelengths corresponding to Chl *a* absorption were more strongly attenuated in the Swanbister mat than wavelengths corresponding to BChl *a* absorption (Fig. 4), whereas in the Waulkmill mat both wavelength regions were almost equally attenuated throughout the mat (Fig. 3).

Spectral scalar irradiance profiles in another mat sample from Swanbister Bay, which was densely covered by purple bacteria and characterized by a pink-colored surface, showed a much more pronounced BChl *a* absorption (Fig. 5, upper graph). The spectral irradiance in the wavelength regions of Chl *a* and BChl *a* absorption was already at a depth of 0.8 mm <10% of the downwelling spectral scalar irradiance. From these profiles, the average attenuation spectrum of scalar irradiance over the depth interval of 0–0.8 mm was calculated (Fig. 5, lower graph). The vertical spectral attenuation coefficient (K_0) was highest in the wavelength region between 400 and 550 nm, the region of carotenoid and Chl *a* absorption. The attenuation coefficient of BChl *a* absorption wavelengths was higher than the attenuation coefficient of Chl *a* absorption, indicating higher densities of purple bacteria in this mat. Thus, mats from Swanbister Bay were very heterogeneous and patchy concerning zonation and population densities of oxygenic and especially anoxygenic phototrophs.

In Swanbister Bay mats covered by purple bacteria (pink surface), only a few genera of cyanobacteria, i.e., mainly unicellular morphotypes of the *Pleurocapsa* group and one filamentous type, were found in low numbers (Table 3).

Microbial Community Structure of Swanbister Bay Mats

To assess the microbial community structure of a Swanbister Bay mat, the universal primer pair 8f-926r targeting a partial sequence of the 16S rDNA gene of eubacteria was applied. After digestion with two different restriction enzymes (*Hae*III, *Hin*6I), the diversity of the amplified 16S fragments was analyzed by T-RFLP. The structure of the T-RFLP profiles, as characterized by the number and distribution of major bands (peaks of highest relative fluorescence intensity), varied from top to bottom of the mat (data not shown). Depending on the restriction enzyme used, different dominant T-RFs were observed. Degrees of similarity among the microbial communities of the different mat layers were quantified with the T-RFLP profile matrix program (RDP). The resulting similarity dendrogram (not shown) did not reveal any specific distribution of microbial communities in the analyzed mat layers, probably because several bacterial species may have terminal fragments of identical size.

Table 2. Filamentous and unicellular cyanobacteria in Waulkmill Bay mats tentatively identified according to Castenholz [10] and their characteristics and depth distribution as determined by CLSM and light microscopy

Genera (tentatively)	Diameter (µm)	Septation	Gas vacuoles	Sheath	Abundance	Depth (mm)
Filamentous cyanobacteria						
Lyngbya sp.	6.25–10.30	+	-	+	(+++)	0; 1.85
Oscillatoria sp.	12.5–14	-	-	+	(+++)	0; 1.85
Leptolyngbya sp.	0.94	-	-	+ (thin)	(++)	3.2
Pseudoanabena sp.	2.5	+	+	+ (thin)	(+)	1.85
Genera (tentatively)	**Diameter (µm)**	**Cell division**		**Sheath**	**Abundance**	**Depth (mm)**
Unicellular cyanobacteria						
Pleurocapsa group	2 × 3	Binary fissions in many different planes		+	(+++)	3.2
Gloeocapsa group	4–8	2 or 3 planes		+	(+++)	0; 1.85; 3.2
Microcystis sp.	1.9 × 1.9	Binary fissions in many different planes		+	(++)	0; 1.85; 3.2; 5.1
Aphanothece sp.	5 × 7	1 plane		+ (thin)	(++)	0
Pleurocapsa group	Diverse size and form	Binary fissions in several planes (pseudofilaments)		-	(+)	1.85

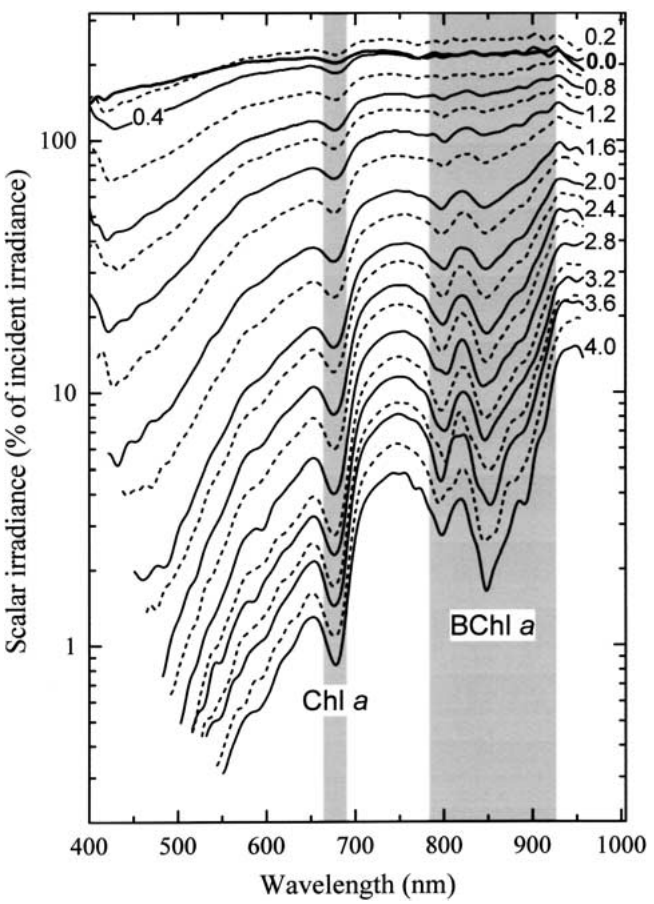

Fig. 4. Depth profile of spectral scalar irradiance in a Swanbister Bay mat normalized to the downwelling spectral scalar irradiance at the mat surface. Numbers indicate depth (mm).

More specific primers were used to analyze the sulfate-reducing and anoxygenic phototrophic microbial community. The biodiversity of the sulfate-reducing bacteria (SRB) was analyzed using the primers 8f-SRB385 and the combination of both restriction enzymes (*Hae*III, *Hin*6I). The resulting T-RFLP profiles contained almost 60 different peaks. In almost all mat layers fragments of 64, 189, 190, 191, 193, 200, 204 bp were found after digestion with *Hae*III, as well as dominant fragments of 64, 87, 89, 92, 337, 348, 350, 352, 371 bp using *Hin*6I (data not shown). Some T-RFs, however, showed a depth-dependent distribution, as T-RFs obtained with *Hae*III of 178, 181, 182, 209, 267, 314 and 317 bp were predominating only in the upper mat layers, whereas T-RFs of 268, 312, 315 bp were dominant in layers below 1 mm depth (data not shown). A similarity dendrogram was obtained by comparing all T-RFs observed with the two different restriction enzymes in each mat layer (Fig. 6A), which indicated a stratification of the SRB communities. The SRB communities in the upper mat layer (0–1 mm) seemed to be related and formed a distinct cluster, clearly differing from the ones at increasing depths. Two other closely related groups were located between 1 and 1.6 mm and between 2 and 3 mm depth, suggesting two different communities of SRB in these depth horizons. Furthermore, populations of SRB in the layer at 1.6–2 mm depth seem to form a divergent cluster.

The T-RFLP patterns were analyzed by Canonical Correspondence Analysis to reveal the variables, which influenced the organization of each SRB population.

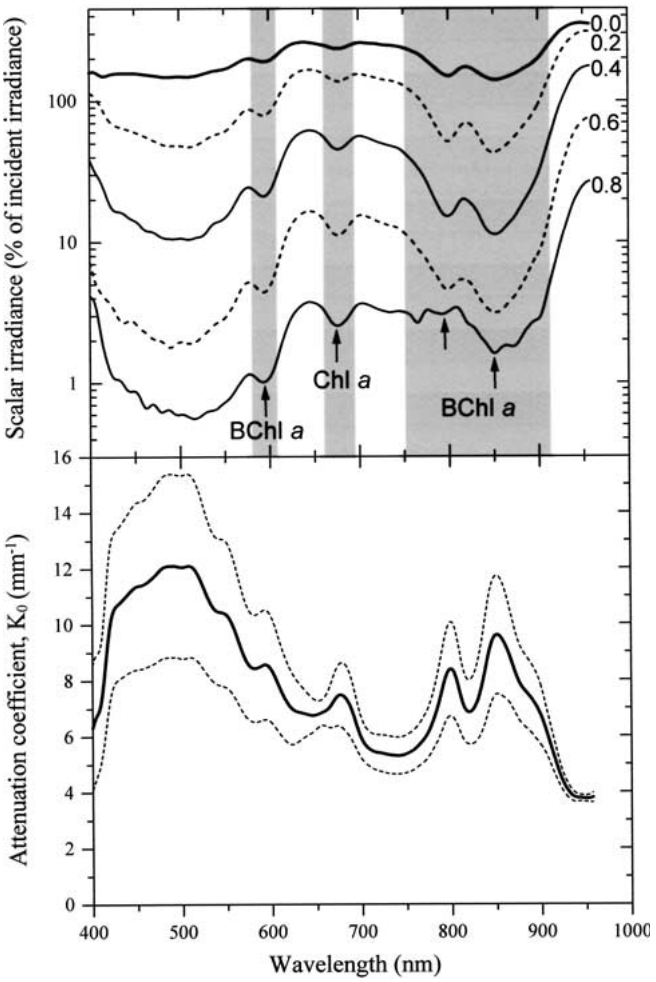

Fig. 5. Depth profile of spectral scalar irradiance (upper graph) in a Swanbister Bay mat densely covered by purple bacteria. The profiles of spectral scalar irradiance were normalized to the downwelling spectral scalar irradiance at the mat surface. Numbers indicate depth (mm). Average attenuation spectrum of scalar irradiance over the depth interval of 0–0.8 mm (lower graph), calculated from the spectral scalar irradiance profiles shown in the upper graph. Broken lines in the lower graph indicate the standard deviations of the attenuation coefficients, K_0.

Using the averaged microsensor O_2 profile at 1312 µmol photons $m^{-2}s^{-1}$ and scalar irradiance profiles at Chl *a* (676 nm) and BChl *a* (845 nm) absorption wavelengths in the top 3 mm of the mat (Figs. 4, 7C), this analysis showed that their dispersion was influenced mostly by irradiance and O_2 concentration (Fig. 6C). Two distinct groups appeared, one in the anaerobic zone and one in the aerobic zone exposed to light. This analysis showed a distribution of different SRB species with depth and thus that SRB were displayed according to depth.

The biodiversity of purple anoxygenic phototrophic bacteria (PAB) was assessed by using primers designed to target the *pufM* gene, which is encoding for a subunit of the photosynthetic reaction center in purple sulfur and purple nonsulfur bacteria. T-RFLP analysis of the amplified *pufM* fragments resulted in complex profiles containing about 30 peaks. Major T-RFs were observed, which allowed a comparison and distinction between the different mat layers. In the upper mat layers fragment peaks of 129, 187, 201, and 203 bp were found (*Hae*III), whereas the bottom layers were characterized by fragment peaks of 215 and 225 bp (data not shown).

Similarity dendrograms showed delineation of the profiles into clusters, indicating a stratification of purple phototrophic bacteria within the mat (Fig. 6B). Purple phototrophic communities from 1.4 to 2 mm and from 1–1.4/2–3 mm depth were closely related. These two community clusters were less closely related to the community in the upper mat layers than to the community below 3 mm depth. Furthermore, the similarity dendrogram also suggests that there were significant differences between the anoxygenic phototrophic communities in the uppermost millimeter of the mat.

Canonical correspondence analysis obtained from T-RFLP profiles showed that the phototrophic communities of the upper layers were clearly influenced by irradiance. In contrast, communities of the deep layers were negatively influenced by O_2 penetration (Fig. 6D). Surprisingly, predicted patterns of T-RFs from *pufM* sequences digested with *Hae*III or *Hin*6I obtained from the NCBI bank (data not shown) showed that the T-RFs specific of the upper layers could correspond to aerobic heterotrophic alphaproteobacteria, such as the genus *Sphingomonas*. Indeed, it has been recently demonstrated that this genus possesses the *pufM* gene [6]. T-RFs from deep layers of the mat could correspond to predicted T-RF patterns of purple sulfur bacteria from the genus *Thiocystis* and of purple nonsulfur bacteria from the genus *Rhodomicrobium*. The general T-RF fingerprints observed within the mat could be equivalent to predicted T-RF patterns of gamma-proteobacteria such as members of the genera *Rhodobacter* or *Allochromatium*.

Microenvironment of Swanbister Bay Mats

Profiles of O_2, gross photosynthesis, pH and H_2S were measured at different positions in a Swanbister Bay mat incubated in darkness and at an irradiance of 1312 µmol photons $m^{-2}s^{-1}$ (Fig. 7). During dark incubation, the average O_2 penetration was 0.8 mm and steep gradients of both H_2S and S_{tot} developed below this depth (Fig. 7A).

Table 3. Filamentous and unicellular cyanobacteria in Swanbister Bay mats tentatively identified according to Castenholz [10] and their characteristics and depth distribution as determined by CLSM and light microscopy

Genera (tentatively)	Diameter (μm)	Septation	Gas vacuoles	Sheath	Abundance	Depth (mm)
Filamentous cyanobacteria						
Borzia sp.	1.88 (short filaments)	+	-	+ (thin)	(+)	1.55
Genera (tentatively)	**Diameter (μm)**	**Cell division**		**Sheath**	**Abundance**	**Depth (mm)**
Unicellular cyanobacteria						
Pleurocapsa group (*Microcystis* sp.)	1.9 × 1.9	Binary fissions in many different planes		+	(+++)	0; 1.55; 3.35
Pleurocapsa group	Diverse size and form	Binary fissions in several planes (pseudofilaments)		-	(+++)	0; 1.55; 3.35
Pleurocapsa group (*Stanieria* sp.)	2 × 3	Multiple fissions or in combination with limited (1–3) binary fissions		-	(+)	3.35

A gradual decrease of pH was found in the dark incubated mat, accounting for a decrease of approximately 1 pH unit between the water and the mat at around 4 mm depth (Fig. 7B). Sulfate reduction rates were lowest in the upper centimeter of dark incubated Swanbister Bay mats and highest in the 1–2 cm depth interval (Table 4).

At an irradiance of 1312 μmol photons $m^{-2}s^{-1}$, gross oxygenic photosynthesis occurred in the upper 2.8 mm of the mat, leading to an increased O_2 penetration of 4 mm and a peak of O_2 concentration at 1.6 mm depth (Fig. 7C). As calculated from the profiles of spectral scalar irradiance measured in the same mat sample (Fig. 4), this O_2 maximum occurred in the depth layer of highest Chl *a* absorption, as indicated by the depth profile of the vertical attenuation coefficient, K_0, at 676 nm. Below that zone, both O_2 concentration and K_0 (676 nm) decreased, whereas the attenuation coefficient at 845 nm, indicative for BChl *a* absorption, increased. This indicates an increasing population density of BChl *a*–containing anoxygenic phototrophic bacteria in the anoxic mat layer. The presence of a population of anoxygenic phototrophs in the zone of highest O_2 concentration and Chl *a* absorption was indicated by a peak of K_0 (845 nm) in that zone, which was, however, less pronounced than the peak of K_0 (676 nm).

In the upper 5 mm of the light incubated mat, H_2S was undetectable; only in one position were very low concentrations of H_2S and sulfide detected below 3 mm depth (data not shown). Photosynthetic CO_2 fixation led to an increase of pH in the upper 2 mm of the mat by more than 0.5 pH unit, with the peak of pH located approximately in the layer of maximal O_2 concentration and K_0 (676 nm). At increasing depths the pH decreased to pH 7.5 (Fig. 7D).

Oxygen and Sulfide Cycling as a Function of Irradiance in Swanbister Bay Mats

In the same sediment core, O_2, gross photosynthesis, H_2S and pH profiles were measured at a fixed position at increasing downwelling irradiances (Fig. 8). Oxygen penetration increased in the mat with increasing irradiance from 0.8 mm during darkness to 1.4, 1.6, 2.2, and 2.6 mm at 43, 96, 183, and 349 μmol photons $m^{-2}s^{-1}$, respectively. At an irradiance of 96 μmol photons $m^{-2}s^{-1}$, a net production of O_2 was detected. The thickness of the photic zone increased gradually from 0.5 mm at 43 μmol photons $m^{-2}s^{-1}$ to 1.8 mm at 349 μmol photons $m^{-2}s^{-1}$ (Fig. 8, upper panel). The increase of gross oxygenic photosynthesis and of the photic zone thickness with irradiance led to a gradual increase of pH in the upper mat layers (Fig. 8, lower panel). The pronounced pH maximum in the upper mat layer at irradiances >43 μmol photons $m^{-2}s^{-1}$ affected the corresponding S_{tot} profiles (Fig. 8, upper panel). Profiles of S_{tot} were calculated from measured H_2S and pH profiles. The S_{tot} profiles at these irradiances showed a pronounced shoulder of S_{tot} concentration, which was not present in the corresponding H_2S profiles and was probably caused by the curvature of the pH profiles. Since H_2S and pH profiles could not be measured at exactly the same position, the unusual shape of the S_{tot} profiles was most probably caused by a pronounced microheterogeneity of the mat. These shoulders in the S_{tot} profiles thus represent overestimations of sulfide concentration and will not be discussed further. Compared to the H_2S profile in the dark incubated mat, the upper H_2S boundary moved downward in the mat at irradiances >96 μmol photons $m^{-2}s^{-1}$ (Fig. 8, upper panel).

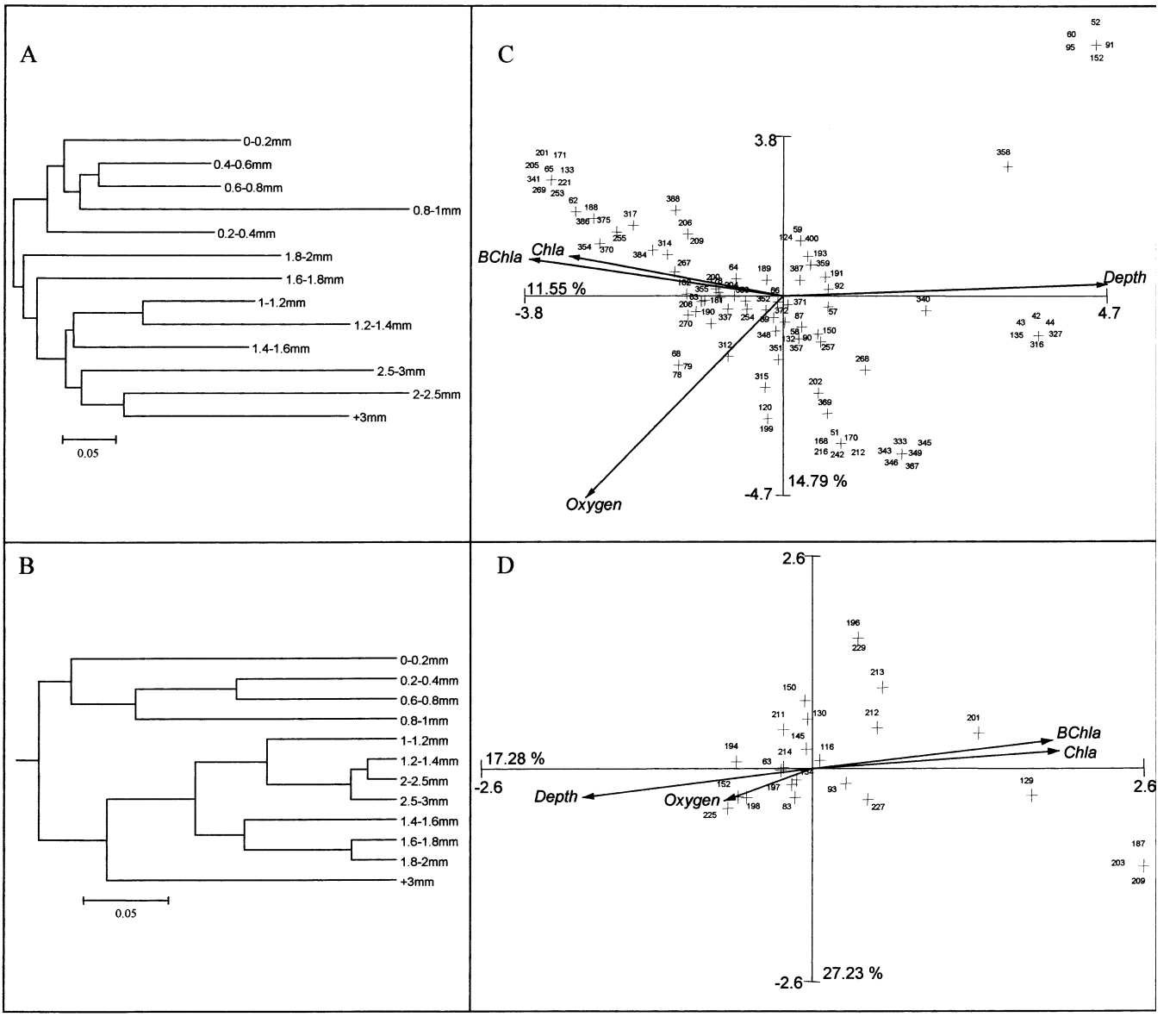

Fig. 6. The sulfate-reducing (SRB) (A) and the purple anoxygenic bacterial (PAB) (B) community relatedness of each layer of a Swanbister Bay mat based on the Jaccard coefficient. Each community was represented by a phylogenetic signature constructed by stacking two individual 5′ T-RFLP patterns corresponding to the *Hae*III and *Hin*6I digests of the 16S rRNA encoding gene for the SRB and the *pufM* gene for the PAB. Canonical correspondence analysis (CCA) between SRB (C) or PAB (D) (T-RF in base pairs) and environmental variables: scalar irradiance at characteristic Chl *a* (676 nm) and BChl *a* (845 nm) absorption wavelengths, O_2 concentration, and depth.

Areal rates of net oxygenic photosynthesis (P_n), calculated as the O_2 flux across the mat–water interface, rates of O_2 consumption in the aphotic zone (R_{aphot}), and rates of H_2S oxidation/production (H_2S fluxes) increased with irradiance and saturated at higher irradiances (Fig. 9). The determined H_2S fluxes, however, strongly underestimate sulfide fluxes, since pH also tends to increase in deeper layers at higher irradiance, which results in calculation of higher sulfide concentrations from H_2S data. Increasing H_2S fluxes will therefore translate to much stronger increases of sulfide fluxes.

Discussion

Microbial Community Composition of Waulkmill and Swanbister Bay Mats

In mats from both Waulkmill and Swanbister Bay, the presence of oxygenic phototrophs was evident (Figs. 1, 2,

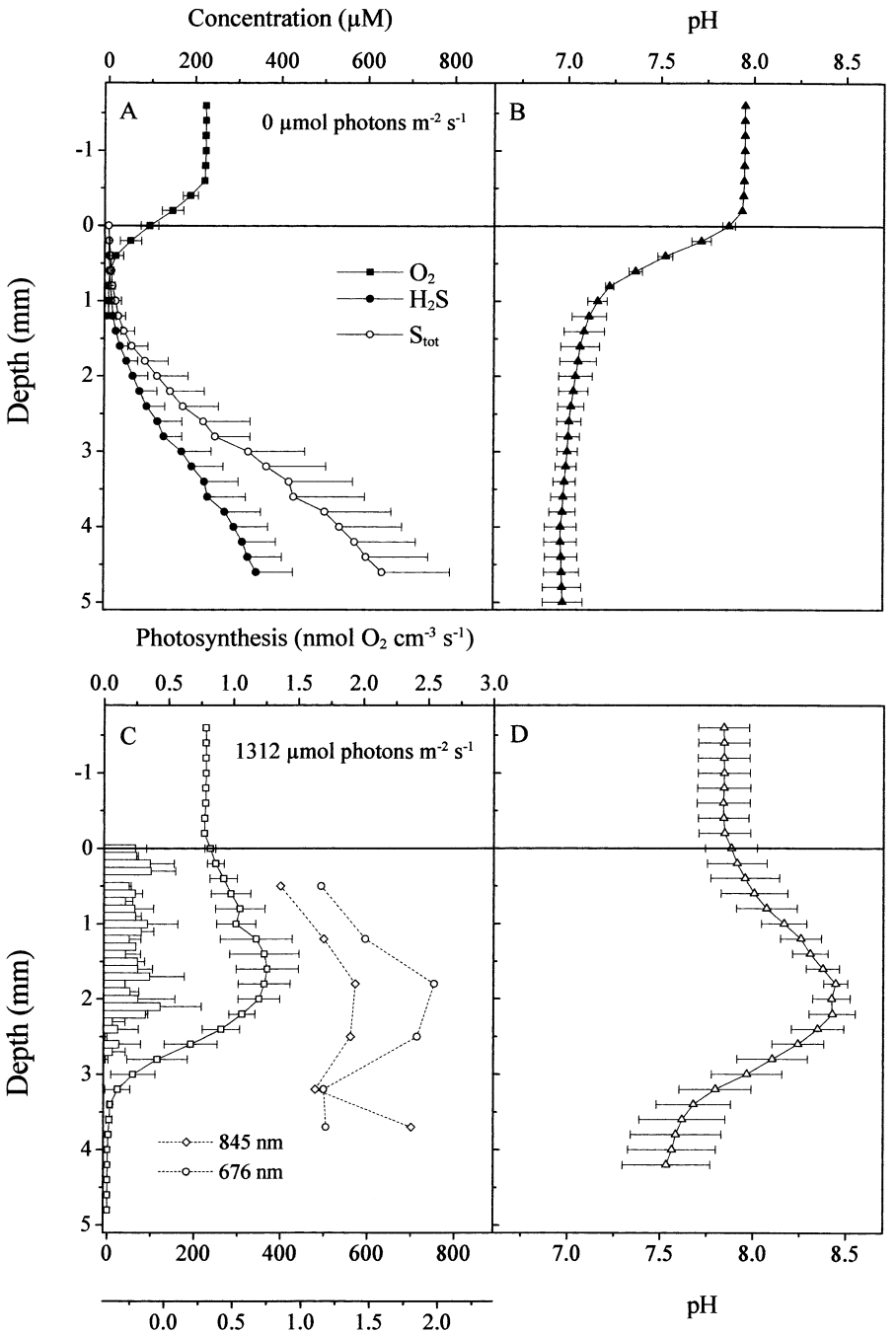

Fig. 7. Average profiles (n = 2–3) of gross photosynthesis (bars), O_2, H_2S, sulfide (S_{tot}) (A, C), and pH (B, D) measured at different positions in a Swanbister Bay mat at 0 (A, B) and 1312 µmol photons $m^{-2}s^{-1}$ (C, D). Error bars indicate standard deviation. Depth profiles of the vertical attenuation coefficient, K_0, at characteristic Chl *a* (676 nm) and BChl *a* (845 nm) absorption wavelengths as calculated from the depth profiles of spectral scalar irradiance measured in the same mat sample (profiles shown in Fig. 4).

3, 4, Tables 2, 3). Biomarker and CLSM analysis revealed a more pronounced abundance of cyanobacteria and high amounts of algal lipids (phytol, sterols, alkenones, highly branched isoprenoid hydrocarbons, heptadecane, and heptadecenes) in Waulkmill Bay mats. This indicates high contributions of oxygenic phototrophs in Waulkmill Bay mats, with specific contributions from diatoms and Haptophyceae. The latter were most probably of planktonic origin, buried in the sediment after settling on the sediment surface.

The bio-optical properties of two different Swanbister Bay mat samples revealed a strong heterogeneity concerning the phototrophic community (Figs. 4, 5), indicating a pronounced patchiness of the distribution of purple bacteria on Swanbister beach. A factor influencing the distribution and population densities of purple sulfur bacteria can be the availability of sulfide. The amount of sulfide present in the mat will limit the presence of oxygenic phototrophs to species able to cope with temporary exposure to sulfide. Environmental conditions on beaches

Table 4. Depth distribution of average sulfate reduction rates (n = 2–3) in Swanbister Bay mats

Depth (cm)	Sulfate reduction rate (nmol $cm^{-3}d^{-1}$)
0–1	234 ± 58
1–2	297 ± 33
2–3	245 ± 56

in Scapa Flow are restrictive for the development of cyanobacteria, as indicated by the low abundances and few genera found (Tables 2, 3). The production of sulfide by sulfate-reducing bacteria is, among other environmental parameters, controlled by the amount and quality of organic matter in the sediment (e.g., [78]). The main sources of organic matter are decomposing macroalgae buried in the sediment [31], resulting in a heterogeneous distribution of low molecular weight organic substrates for sulfate-reducing bacterial activity.

A pronounced microheterogeneity of sulfate reduction and sulfide distribution was found in Swanbister beach mats, as indicated by the standard deviations of measured sulfate reduction rates and sulfide microprofiles (Table 4, Fig. 7A). Thus, a heterogeneous distribution of sulfide could affect the distribution of the different phototrophs. A patchy distribution of sites virtually covered by purple bacteria (pink surface) was observed on Swanbister beach during sampling in July 2000, as well as a patchy distribution of macroalgae growing on the beach or deposited on the sediment surface. Additional to organic matter supply after decomposition, organic sulfur compounds such as dimethylsulfide (DMS) and dimethylsulfoniopropionate (DMSP) might be released from degrading macroalgae. Both compounds are potential substrates for purple bacteria [39], including *Thiocapsa roseopersicina* [90, 37, 38]. By providing such organic sulfur substrates, degrading macroalgae could also directly enhance growth of purple sulfur bacteria in their nearby surroundings, further contributing to their patchy distribution on these beaches.

Biomarker analysis showed that lipids reflecting the presence of methanogens (phytenes and 2,6,10,15,19-

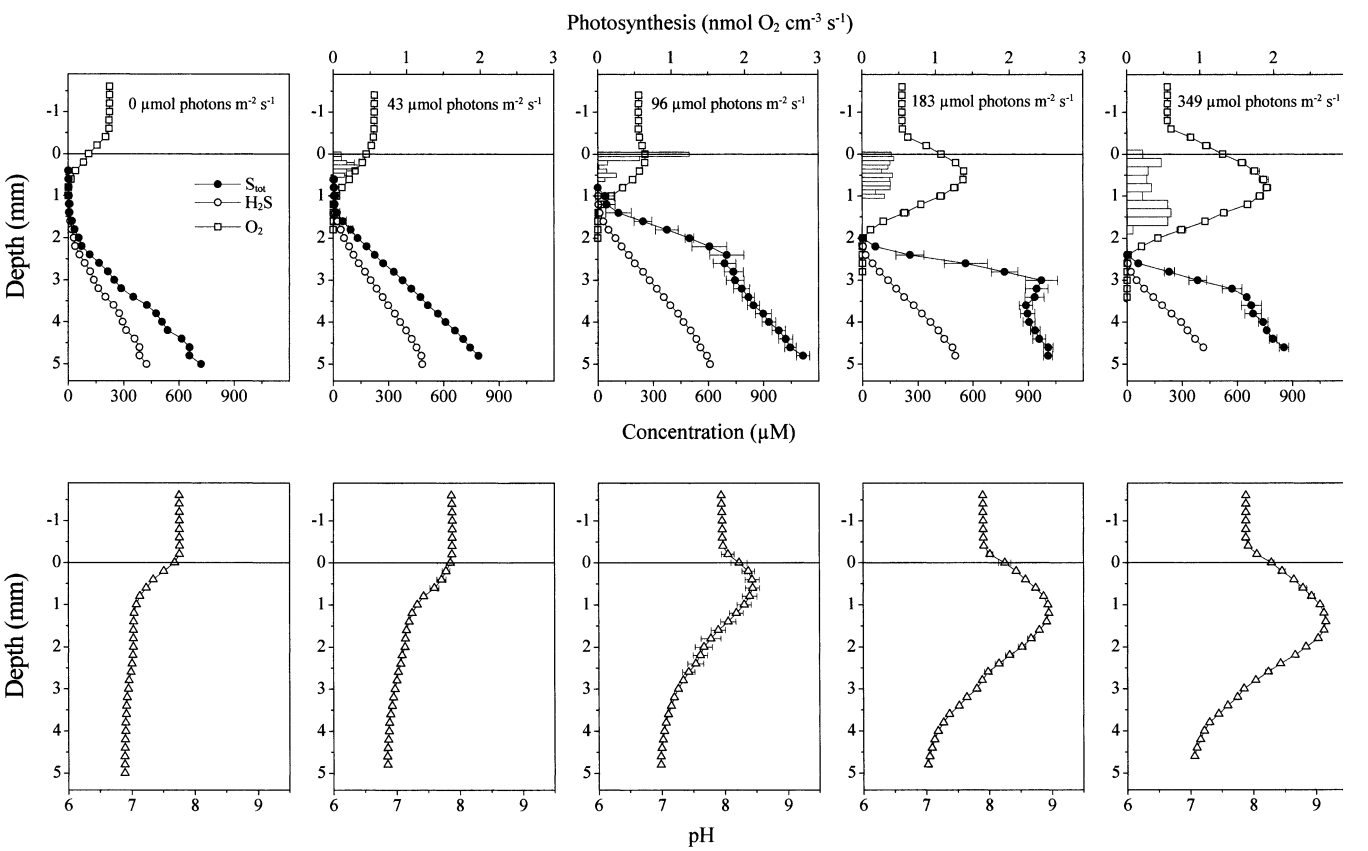

Fig. 8. Average profiles (n = 1–3) of gross photosynthesis (bars), O_2, H_2S, sulfide (S_{tot}) (upper panel) and pH (lower panel) measured at a fixed position in the same mat from Swanbister Bay at increasing downwelling irradiances. Error bars indicate standard deviation.

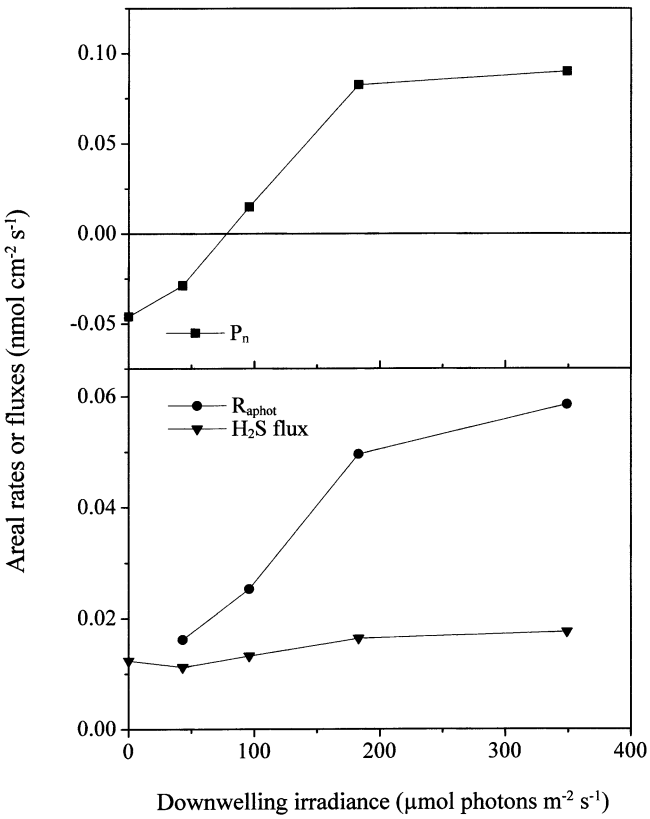

Fig. 9. Areal rates of net photosynthesis (P_n), O_2 consumption in the aphotic zone (R_{aphot}) and of net H_2S production/consumption (H_2S flux) vs irradiance in the Swanbister Bay mat.

pentamethylicosane), as well as fatty acids characteristic of sulfate-reducing bacteria (*iso*- and *anteiso*-pentadecanoic acids) were abundant especially in Swanbister Bay mats (Fig. 1). With our data we can, however, only speculate on the biogeochemical importance of methanogens in the mat. As has been shown in salt marsh sediments (e.g., [66, 76]), methane production in marine sediments is most probably due to utilization of noncompetitive substrates such as methylamines and DMS [43, 65]. Glycine betaine, one of the most widespread compatible solutes [94], and the osmoregulatory compound of marine algae, DMSP [42], present at high concentrations in microbial mats [39, 89], are precursors of trimethylamine and DMS [65]. Thus, these compounds could potentially play a role as substrates for methanogenesis in these mats.

Oxygen and Sulfur Cycling in Swanbister Bay Mats

Microsensor data showed a gradual increase of both O_2 concentration and penetration with irradiance due to increasing oxygenic photosynthesis by cyanobacteria and microalgae in Swanbister Bay mats (Figs. 8, 9). Furthermore, H_2S fluxes tended to increase with irradiance (Fig. 9), indicating higher sulfide turnover rates in light conditions. These include both higher production rates by sulfate reduction and higher sulfide consumption rates. Although (aerobic) chemolithotrophic sulfide oxidation by *T. roseopersicina* may occur in light conditions [70, 71], phototrophic oxidation (in the presence of O_2) seem to be preferred because of higher energetic yields by phototrophy than by chemotrophy [17, 84, 85]. The light dependency of the H_2S fluxes (Fig. 9) further suggests that anoxygenic photosynthesis by purple sulfur bacteria strongly affected net H_2S consumption in light-incubated Swanbister beach mats.

Microsensor data on sulfide cycling underestimate sulfur cycling in microbial mats, since fluxes calculated from microprofiles represent only net rates of sulfide turnover. As has been shown in light-incubated cyanobacterial mats [9, 88, 77], sulfate reduction can occur in the highly oxygenated surface layer. This activity, however, is not detectable with H_2S microsensors because of immediate reoxidation of the produced sulfide. Furthermore, other reduced sulfur compounds, such as polysulfides, elemental sulfur, and thiosulfate, which are present in Swanbister mats [86], may play a significant role in the sulfur cycle of these mats. The dominant purple sulfur bacterium in these mats, *T. roseopersicina*, is characterized by a high metabolic versatility [69, 84] and can use polysulfide [87], thiosulfate [17], and intracellular elemental sulfur [70, 71].

Oxygen consumption rates in the aphotic zone (R_{aphot}) increased with irradiance (Fig. 9). Although H_2S fluxes underestimate sulfide fluxes especially in light conditions (see Results), aerobic/oxic sulfide oxidation seemed not to have significantly contributed to R_{aphot} at higher irradiances. This points to a more important role of other O_2-consuming processes, such as aerobic respiration. T-RFLP analysis together with predicted patterns of T-RFs supplied from the NCBI Bank indicated the presence of aerobic, heterotrophic alpha-proteobacteria in the upper layers of the mat, which could have contributed to O_2 consumption in that zone. As mentioned by Nagashima et al. [60], the detection of these nonphototrophic bacteria with the primer set targeting specifically the *pufM* gene conserved among purple phototrophic bacteria could be due to horizontal gene transfer. T-RFLP analysis also revealed the presence of different communities of SRB in the uppermost layers of Swanbister Bay mats (Fig. 6A). Sul-

fate-reducing bacteria are also characterized by their capacity for aerobic respiration [47, 81] and could have directly contributed to O_2 consumption in these mat layers.

Communities of Sulfate-Reducing and Purple Bacteria in Swanbister Bay Mats

The populations of purple bacteria within the upper millimeters of the Swanbister mat (Figs. 4, 6B, 7C) experienced pronounced variations of microenvironmental conditions between dark–light transitions (Fig. 8). A minor population in the surface layer experienced highly oxic conditions during light periods and micro-oxic conditions during the night, with sulfide being available only during the night at low concentrations (Figs. 7A, 8). Populations in the depth interval between the surface layer and the permanently anoxic zone (Figs. 7C, 8) were only exposed to sulfide during darkness. In light, these populations experience, at least temporarily, simultaneously low O_2 and sulfide concentrations, since the depth of the oxygen–sulfide interface increased with increasing irradiance (Fig. 8). This condition is subsequently followed by exposure to either solely O_2 or sulfide at further increasing or decreasing irradiances. Populations present below this transition zone always experienced sulfide, but may have been light limited (Fig. 4). Thus, the full spectrum of metabolic versatility may be used by different populations of *T. roseopersicina* zonated in the mats. This includes chemolithotrophy during darkness using O_2 and sulfide as substrates, degradation of storage carbohydrates (glycogen) under anoxic dark conditions, photolithotrophy in the light in the presence of only sulfide, of both sulfide and O_2, or of only O_2 using intracellular elemental sulfur or other external reduced sulfur compounds [69, 84].

A pronounced diversity and a depth-dependent distribution of purple bacteria was found by T-RFLP analysis (Fig. 6B). From *pufM* T-RFLP profiles, a T-RF of 93 bp (restriction enzyme *Hae*III) was detected in all mat layers within the top 3 mm of the mat. The sequences of the *pufL* and *pufM* genes of *T. roseopersicina* strain T. ork were recently determined (A. Fourçans, R. Duran, P. Caumette, unpublished; accession number AJ544223), and a predictive T-RF of 92 bp was found for the *pufM* gene of *T. roseopersicina* digested with this restriction enzyme. So, the observed T-RF could correspond to the predominant purple sulfur bacterium *T. roseopersicina*.

The results also show that in Swanbister mats different communities of anoxygenic phototrophs are zonated within the mat in response to the microenvironmental conditions (Fig. 6D). The predominant T-RF of 214 bp obtained with restriction enzyme *Hin*6I represents the dominating anoxygenic phototrophic community in Swanbister beach mats, as deduced from the sequences and T-RFs of purple bacteria presently available. Although predictive digestions made *in silico* on the RDP Web site (TAP: T-RFLP Analysis Program) cannot be used for phylogenetic identification of communities based on their T-RFs [58], this T-RF could be related to the species *Allochromatium vinosum*. The presence of this major species seemed to be independent of depth, O_2 and irradiance (Fig. 6D) and was distributed all over the mat (data not shown). This species was also found by van Gemerden et al. [86]. Further determination of *pufM* gene sequences from isolated purple bacteria will be useful to obtain more information about the dominant members.

Two closely related community clusters of purple bacteria were found in the depth layer from 1 to 3 mm (Fig. 6B), i.e., in the transition layer of the mat. Communities present in this layer experienced pronounced variations, ranging from highly oxic during high light conditions to sulfidic conditions during darkness. These pronounced variations seem to select for versatile species of purple bacteria (also others than *T. roseopersicina*) able to thrive under these conditions. As indicated by T-RFLP analysis, these could include species of the genus *Allochromatium*, which are characterized by a pronounced metabolic versatility [40, 69].

Since microsensor and T-RFLP analyses were not performed in exactly the same Swanbister mat sample, some deviations concerning the localization of this transition layer might have occurred between both samples. Furthermore, the O_2 and sulfide microgradients measured in a laboratory under controlled conditions similar to the conditions during immersion periods might change during emersion periods as occurring *in situ* during low tide. However, our laboratory microsensor data compare relatively well to microsensor profiles measured *in situ* at low tide by van Gemerden et al. [86]. Furthermore, the fact that these two community clusters were less related to the community in the upper mat layers than to the community below 3 mm depth points to an O_2-dependent distribution of purple bacteria in Swanbister Bay mats. This is consistent with the CCA showing that O_2 is the most important variable influencing the distribution of purple bacteria. Thus, despite the predominance of *T. roseopersicina* in these mats, a variety of different

purple bacteria may have stratified in response to O_2 and sulfide gradients.

Also, the distribution and diversity of sulfate-reducing bacteria seemed to be partly influenced by O_2. A distinct and related SRB community cluster was found in the uppermost mat layer, clearly differing from the communities found at increasing depths (Fig. 6A). Thus, the almost permanent oxic conditions in the uppermost mat layer (Figs. 7, 8) may select for especially O_2-tolerant SRB species. Communities of SRB below this layer are exposed to anaerobic conditions at least during low light and dark periods (Figs. 7, 8). Several SRB, e.g., *Desulfovibrio* species and *Desulfonema*-related bacteria, possess adaptive strategies for survival under oxic conditions, enabling them to thrive in microbial mats. These strategies include aggregation, migration, aerotaxis, and O_2 respiration [46, 47, 81, 22, 59, 77, 14].

The CCA demonstrated that factors other than the presence of O_2 also influenced the depth distribution and diversity of SRB. The influence of irradiance at Chl *a* and BChl *a* absorption wavelengths (Fig. 6C) could be the result of interactions between phototrophs and SRB and might be considered as an indirect irradiance effect. The finding of some groups at different depths was not directly correlated with O_2 or sulfide gradients. Sulfate-reducing bacteria are characterized by a pronounced metabolic versatility and are apparently able to catalyze all reactions of a complete sulfur cycle [13, 14]. This includes the use of a variety of electron acceptors such as sulfite, sulfur, thiosulfate, nitrate, nitrite, O_2, and Fe(III), as well as their ability to perform disproportionation and oxidation of diverse sulfur compounds (sulfur, thiosulfate, sulfite), and aerobic respiration [3, 44, 19, 15, 12, 55, 45, 26, 95]. Thus, not only the presence of O_2 and the availability of organic substrates, but also the distribution of sulfur compounds like thiosulfate, sulfur, and sulfite could influence the distribution of SRB in this mat.

Microbial communities of coastal microbial mats on the Orkney Islands are apparently more diverse than previously described. Furthermore, although mats on Swanbister beach could be distinguished concerning population density and localization of the purple layer on or below the mat surface (Figs. 4, 5), a clear differentiation between different microbial mats as found and described earlier [86] was not possible in July 2000. In particular, sediments populated only by purple bacteria and characterized by an absence of Chl *a*–containing oxygenic phototrophs could not be found. This type of mat was previously described as one of the three types of mat systems developing especially on Swanbister beach [86]. The enforcement of strict waste discharge regulations has led to improved wastewater treatment in the area over the past decade, which has significantly reduced the amount of organic matter discharged onto the beaches. These changes have created environmental conditions less favorable for the exclusive development of purple sulfur bacteria, which would also account for the increased microbial diversity in these mat sediments.

Acknowledgements

We acknowledge the financial support by the EC (MAT-BIOPOL project, grant EVK3-CT-1999-00010) and the Danish Natural Science Research Council (M.K., contract no. 9700549). The staff and especially Alex Simpson, Director of the Orkney County Council Marine Unit laboratory, are gratefully acknowledged for providing excellent laboratory facilities. Anni Glud is acknowledged for the construction of the microsensors.

References

1. Achenbach LA, Carey J, Madigan MT (2001) Photosynthetic and phylogenetic primers for detection of anoxygenic phototrophs in natural environments. Appl Environ Microbiol 67:2922–2926
2. Amann RI, Binder BJ, Olson RJ, Chisholm SW, Devereux R, Stahl DA (1990) Combination of 16S rRNA-targeted oligonucleotide probes with flow cytometry for analyzing mixed microbial populations. Appl Environ Microbiol 56:1919–1925
3. Bak F, Cypionka H (1987) A novel type of energy metabolism involving fermentation of inorganic sulphur compounds. Nature 326:891–892
4. Ballantine JA, Lavis A, Morris RJ (1979) Sterols of the phytoplankton—effects of illumination and growth stage. Phytochemistry 18:1459–1466
5. Barbe A, Grimalt JO, Pueyo JJ, Albaigés J (1990) Characterization of model evaporitic environments through the study of lipid components. Org Geochem 16:815–828
6. Béjà O, Suzuki MT, Heidelberg JF, Nelson WC, Preston CM, Hamada T, Eisen JA, Fraser CM, DeLong EF (2002) Unsuspected diversity among marine aerobic anoxygenic phototrophs. Nature 415:630–633
7. Blumer M, Guillard RRL, Chase T (1971) Hydrocarbons of marine phytoplankton. Mar Biol 8:183–189
8. Broecker WS, Peng T-H (1974) Gas exchange rates between air and sea. Tellus 26:21–35

9. Canfield DE, Des Marais DJ (1991) Aerobic sulfate reduction in microbial mats. Science 251:1471–1473
10. Castenholz RW (2001) Phylum BX. Cyanobacteria. Oxygenic photosynthetic bacteria. In: Boone DR, Castenholz RW (Eds.) Bergey's Manual of Systematic Bacteriology. The Archea and the Deeply Branching and Phototrophic Bacteria, vol 1. Springer, Berlin, pp 473–599
11. Chuecas L, Riley JP (1969) Component fatty acids of the total lipids of some marine phytoplankton. J Mar Biol Assoc UK 49:97–116
12. Coleman ML, Hedrick DB, Lovley DR, White DC, Pye K (1993) Reduction of Fe(III) in sediments by sulphate-reducing bacteria. Nature 361:436–438
13. Cypionka H (1994) Novel metabolic capacities of sulfate-reducing bacteria, and their activities in microbial mats. In: Stal LJ, Caumette P (Eds.) Microbial Mats: Structure, Development and Environmental Significance, NATO ASI Series G, vol 35. Springer, Berlin, pp 367–376
14. Cypionka H (2000) Oxygen respiration by *Desulfovibrio* species. Ann Rev Microbiol 54:827–848
15. Dannenberg S, Kroder M, Dilling W, Cypionka H (1992) Oxidation of H_2, organic compounds and inorganic sulfur compounds coupled to reduction of O_2 or nitrate by sulfate-reducing bacteria. Arch Microbiol 158:93–99
16. de Wit R, Jonkers HM, van den Ende FP, van Gemerden H (1989) *In situ* fluctuations of oxygen and sulphide in marine microbial sediment ecosystems. Neth J Sea Res 23:271–281
17. de Wit R, van Gemerden H (1987) Chemolithotrophic growth of the phototrophic sulfur bacterium *Thiocapsa roseopersicina*. FEMS Microbiol Ecol 45:117–126
18. Didyk BM, Simoneit BRT, Brassell SC, Eglinton G (1978) Organic geochemical indicators of palaeoenvironmental conditions of sedimentation. Nature 272:216–222
19. Dilling W, Cypionka H (1990) Aerobic respiration in sulfate-reducing bacteria. FEMS Microbiol Lett 71:123–128
20. Eglinton G, Hamilton RJ (1967) Leaf epicuticular waxes. Science 156:1322
21. Epping EHG, Khalili A, Thar R (1999) Photosynthesis and the dynamics of oxygen consumption in a microbial mat as calculated from transient oxygen microprofiles. Limnol Oceanogr 44:1936–1948
22. Eschemann A, Kühl M, Cypionka H (1999) Aerotaxis in *Desulfovibrio*. Environ Microbiol 1:489–495
23. Fonselius SH (1983) Determination of hydrogen sulphide. In: Grasshoff K, Ehrhardt M, Kremling K (Eds.) Methods of Seawater Analysis. Verlag Chemie, Weinheim, pp 73–80
24. Fossing H, Jørgensen BB (1989) Measurement of bacterial sulfate reduction in sediments: evaluation of a single-step chromium reduction method. Biogeochemistry 8:205–222
25. Fromin N, Hamelin J, Tarnawski S, Roesti D, Jourdain-Miserez K, Forestier N, Teyssier-Cuvelle S, Gillet F, Aragno M, Rossi P (2002) Statistical analysis of denaturing gel electrophoresis (DGE) fingerprinting patterns. Environ Microbiol 4:634–643
26. Fuseler K, Krekeler D, Sydow U, Cypionka H (1996) A common pathway of sulfide oxidation by sulfate-reducing bacteria. FEMS Microbiol Lett 144:129–134
27. García HE, Gordon LI (1992) Oxygen solubility in seawater: Better fitting equations. Limnol Oceanogr 37:1307–1312
28. Grant J, Gust G (1987) Prediction of coastal sediment stability from photopigment content of mats of purple sulphur bacteria. Nature 330:244–246
29. Grimalt JO, de Wit R, Teixidor P, Albaiges J (1992) Lipid biogeochemistry of *Phormidium* and *Microcoleus* mats. Org Geochem 19:509–530
30. Han J, McCarthy ED, Calvin M, Benn MH (1968) Hydrocarbon constituents of the blue-green algae *Nostoc muscorum*, *Anacystis nidulans*, *Phormidium luridum* and *Chlorogloea fritschii*. J Chem Soc C:2785–2791
31. Herbert RA (1985) Development of mass blooms of photosynthetic bacteria on sheltered beaches in Scapa Flow, Orkney Islands. Proc Roy Soc Edinburgh 87B:15–25
32. Hershey JP, Plese T, Millero FJ (1988) The pK_1* for the dissociation of H_2S in various ionic media. Geochim Cosmochim Acta 52:2047–2051
33. Hoffmann C (1942) Beiträge zur Vegetation des Farbstreifen-Sandwattes. Kieler Meeresforschungen Sonderheft 4:85–108
34. Holzer G, Oro J, Tornabene TG (1979) Gas chromatographic–mass spectrometric analysis of neutral lipids from methanogenic and thermoacidophilic bacteria. J Chromatogr 186:795–809
35. Isaksen M, Finster K (1996) Sulfate reduction in the root zone of the sea grass *Zostera noltii* on the intertidal flats of a coastal lagoon (Arcachon, France). Mar Ecol Prog Ser 137:187–194
36. Jeroschewski P, Steuckart C, Kühl M (1996) An amperometric microsensor for the determination of H_2S in aquatic environments. Anal Chem 68:4351–4357
37. Jonkers HM, de Bruin S, van Gemerden H (1998) Turnover of dimethylsulfoniopropionate (DMSP) by the purple sulfur bacterium *Thiocapsa roseopersicina* M11: ecological implications. FEMS Microbiol Ecol 27:281–290
38. Jonkers HM, Jansen M, Van der Maarel MJEC, van Gemerden H (1999) Aerobic turnover of dimethyl sulfide by the anoxygenic phototrophic bacterium *Thiocapsa roseopersicina*. Arch Microbiol 172:150–156
39. Jonkers HM, Koopmans GF, van Gemerden H (1998) Dynamics of dimethyl sulfide in a marine microbial mat. Microb Ecol 36:93–100
40. Kämpf C, Pfennig N (1980) Capacity of Chromatiaceae for chemotrophic growth. Specific respiration rates of *Thiocystis violacea* and *Chromatium vinosum*. Arch Microbiol 127:125–135
41. Kates M, Tremblay P, Anderson R, Volcani BE (1978) Identification of the free and conjugated sterol in a non-photosynthetic diatom, *Nitzschia alba*, as 24-methylene cholesterol. Lipids 13:34–41

42. Kelly DP, Smith NA (1990) Organic sulfur compounds in the environment. Adv Microb Ecol 11:345–385
43. King GM (1984) Utilisation of hydrogen, acetate and "non-competitive" substrates by methanogenic bacteria in marine sediments. Geomicrobiol J 3:275–306
44. Krämer M, Cypionka H (1989) Sulfate formation via ATP sulfurylase in thiosulfate- and sulfite-disproportionating bacteria. Arch Microbiol 151:232–237
45. Krekeler D, Cypionka H (1995) The preferred electron acceptor of *Desulfovibrio desulfuricans* CSN. FEMS Microbiol Ecol 17:271–278
46. Krekeler D, Sigalevich P, Teske A, Cypionka H, Cohen Y (1997) A sulfate-reducing bacterium from the oxic layer of a microbial mat from Solar Lake (Sinai), *Desulfovibrio oxyclinae* sp. nov. Arch Microbiol 167:369–375
47. Krekeler D, Teske A, Cypionka H (1998) Strategies of sulfate-reducing bacteria to escape oxygen stress in a cyanobacterial mat. FEMS Microbiol Ecol 25:89–96
48. Kühl M, Fenchel T (2000) Bio-optical characteristics and the vertical distribution of photosynthetic pigments and photosynthesis in an artificial cyanobacterial mat. Microb Ecol 40:85–93
49. Kühl M, Jørgensen BB (1992) Spectral light measurements in microbenthic phototrophic communities with a fiber-optic microprobe coupled to a sensitive diode array detector. Limnol Oceanogr 37:1813–1823
50. Kühl M, Steuckart C, Eickert G, Jeroschewski P (1998) A H_2S microsensor for profiling biofilms and sediments: application in an acidic lake sediment. Aquat Microb Ecol 15:201–209
51. Kumar S, Tamura K, Jakobsen IB, Nei M (2001) MEGA2: Molecular evolutionary genetics analysis software, Bioinformatics
52. Lassen C, Ploug H, Jørgensen BB (1992) A fibre-optic scalar irradiance microsensor: Application for spectral light measurements in sediments. FEMS Microbiol Ecol 86:247–254
53. Li Y-H, Gregory S (1974) Diffusion of ions in sea water and in deep-sea sediments. Geochim Cosmochim Acta 38:703–714
54. Liu WT, Marsh TL, Cheng H, Forney LJ (1997) Characterization of microbial diversity by determining terminal restriction fragment length polymorphisms of genes encoding 16S rRNA. Appl Environ Microbiol 63:4516–4522
55. Lovley DR, Phillips EJP (1994) Novel processes for anaerobic sulfate production from elemental sulfur by sulfate-reducing bacteria. Appl Environ Microbiol 60:2394–2399
56. Maidak BL, Cole JR, Lilburn TG, Parker CTJ, Saxman PR, Farris RJ, Garrity GM, Olsen GJ, Schmidt TM, Tiedje JM (2001) The RDP-II (Ribosomal Database Project). Nucleic Acids Res 29:173–174
57. Marlowe IT, Brassell SC, Eglinton G, Green JC (1984) Long chain unsaturated ketones and esters in living algae and marine sediments. Org Geochem 6:135–141
58. Marsh TL, Saxman P, Cole J, Tiedje J (2000) Terminal restriction fragment length polymorphism analysis program, a web-based research tool for microbial community analysis. Appl Environ Microbiol 66:3616–3620
59. Minz D, Flax JL, Green SJ, Muyzer G, Cohen Y, Wagner M, Rittmann BE, Stahl DA (1999) Diversity of sulfate-reducing bacteria in oxic and anoxic regions of a microbial mat characterized by comparative analysis of dissimilatory sulfite reductase genes. Appl Environ Microbiol 65:4666–4671
60. Nagashima KVP, Hiraishi A, Shimada K, Matsuura K (1997) Horizontal transfer of genes coding for the photosynthetic reaction centers of purple bacteria. J Mol Evol 45:131–136
61. Nes WR, McKean ML (1977) Biogeochemistry of Steroids and Other Isoprenoids. University Park Press, Baltimore
62. Nichols PD, Volkman JK, Palmisano AC, Smith GA, White DC (1988) Occurrence of an isoprenoid C_{25} diunsaturated alkene and high neutral lipid content in Antarctic sea-ice diatom communities. J Phycol 24:90–96
63. Nishimura M, Koyama T (1977) The occurrence of stanols in various living organisms and the behaviour of sterols in contemporary sediments. Geochim Cosmochim Acta 41:379–385
64. Orcutt DM, Paterson GW (1975) Sterol, fatty acid and elemental composition of diatoms grown in chemically defined media. Comp Biochem Physiol 506:579–583
65. Oremland RS, King GM (1989) Methanogenesis in hypersaline environments. In: Cohen Y, Rosenberg E (Eds.) Microbial Mats: Physiological Ecology of Benthic Microbial Communities. American Society for Microbiology, Washington DC, pp 180–190
66. Oremland RS, Marsh LM, Polcin S (1982) Methane production and simultaneous sulfate reduction in anoxic, salt marsh sediments. Nature 296:143–145
67. Paoletti C, Pushparaj B, Florenzano G, Capella P, Lercker G (1976) Unsaponifiable matter of green and blue-green algal lipids as a factor of biochemical differentiation of their biomass: II. Terpenic alcohol and sterol fractions. Lipids 11:266–271
68. Patterson GW (1974) Sterols of some green algae. Comp Biochem Physiol 47B:453–457
69. Pfennig N, Trüper HG (1992) The family Chromatiaceae. In: Balows A, Trüper HG, Dworkin M, Harder W, Schleifer K-H (Eds.) The Prokaryotes. Springer, Berlin, pp 3200–3221
70. Pringault O, de Wit R, Caumette P (1996) A benthic gradient chamber for culturing phototrophic sulfur bacteria on reconstituted sediments. FEMS Microbiol Ecol 20:237–250
71. Pringault O, de Wit R, Kühl M (1999) A microsensor study of the interaction between purple sulfur and green sulfur bacteria in experimental benthic gradients. Microb Ecol 37:173–184
72. Revsbech NP (1989) An oxygen microelectrode with a guard cathode. Limnol Oceanogr 34:474–478
73. Revsbech NP, Jørgensen BB (1983) Photosynthesis of benthic microflora measured with high spatial resolution by the

oxygen microprofile method: Capabilities and limitations of the method. Limnol Oceanogr 28:749–756
74. Revsbech NP, Jørgensen BB (1986) Microelectrodes: Their use in microbial ecology. Adv Microb Ecol 9:293–352
75. Schouten S, van der Maarel MEJ, Huber R, Sinninghe Damsté JS (1997) 2,6,10,15,19-Pentamethylicosenes in *Methanolobus bombayensis*, a marine methanogenic archaeon and *Methanosarcina mazei*. Org Geochem 26:409–414
76. Senior E, Lindstrom EB, Banat I, Nedwell DB (1982) Sulfate reduction and methanogenesis in the sediment of a saltmarsh on the east coast of the United Kingdom. Appl Environ Microbiol 43:987–996
77. Sigalevich P, Meshorer E, Helman Y, Cohen Y (2000) Transition from anaerobic to aerobic growth conditions for the sulfate-reducing bacterium *Desulfovibrio oxyclinae* results in flocculation. Appl Environ Microbiol 66:5005–5012
78. Skyring GW (1987) Sulfate reduction in coastal ecosystems. Geomicrobiol J 5:295–374
79. Stal LJ, van Gemerden H, Krumbein WE (1985) Structure and development of a benthic marine microbial mat. FEMS Microbiol Ecol 31:111–125
80. Tabatabai MA (1974) Determination of sulfate in water samples. Sulfur Inst J 10:11–14
81. Teske A, Ramsing NB, Habicht K, Fukui M, Küver J, Jørgensen BB, Cohen Y (1998) Sulfate-reducing bacteria and their activities in cyanobacterial mats of Solar Lake (Sinai, Egypt). Appl Environ Microbiol 64:2943–2951
82. Tornabene TG, Langworthy TA, Holzer G, Oro J (1979) Squalenes, phytanes and other isoprenoids as major neutral lipids of methanogenic and thermoacidophilic "archaebacteria." J Mol Evol 13:73–83
83. Ullman WJ, Aller RC (1982) Diffusion coefficients in nearshore marine sediments. Limnol Oceanogr 27:552–556
84. van Gemerden H (1993) Microbial mats: a joint venture. Mar Geol 113:3–25
85. van Gemerden H, de Wit R, Tughan CS, Herbert RA (1989a) Development of mass blooms of *Thiocapsa roseopersicina* on sheltered beaches on the Orkney Islands. FEMS Microbiol Ecol 62:111–118
86. van Gemerden H, Tughan CS, de Wit R, Herbert RA (1989b) Laminated microbial ecosystems on sheltered beaches in Scapa Flow, Orkney Islands. FEMS Microbiol Ecol 62:87–102
87. Visscher PT, Nijburg JW, van Gemerden H (1990) Polysulfide utilization by *Thiocapsa roseopersicina*. Arch Microbiol 155:75–81
88. Visscher PT, Prins RA, van Gemerden H (1992) Rates of sulfate reduction and thiosulfate consumption in a marine microbial mat. FEMS Microbiol Ecol 86:283–294
89. Visscher PT, Quist P, van Gemerden H (1991) Methylated sulfur compounds in microbial mats: in situ concentrations and metabolism by a colorless sulfur bacterium. Appl Environ Microbiol 57(6):1758–1763
90. Visscher PT, van Gemerden H (1991) Photo-autotrophic growth of *Thiocapsa roseopersicina* on dimethyl sulfide. FEMS Microbiol Lett 81:247–250
91. Vogel AI (1978) Textbook of Practical Organic Chemistry. Longman, New York
92. Volkman JK, Eglinton G, Corner EDS, Sargent JR (1980) Novel unsaturated straight-chain C_{37}–C_{39} methyl and ethyl ketones in marine sediments and a coccolithophore *Emiliania huxleyi*. Adv Org Geochem 1979:219–227
93. Volkman JK, Jeffrey SW, Nichols PD, Rogers GI, Garland CD (1989) Fatty acids and lipid composition of 10 species of microalgae used in mariculture. J Exp Mar Biol Ecol 128:219–240
94. Welsh DT (2000) Ecological significance of compatible solute accumulation by microorganisms: from single cells to global climate. FEMS Microbiol Rev 24:263–290
95. Widdel F (1988) Microbiology and ecology of sulfate- and sulfur-reducing bacteria. In: Zehnder AJB (Eds.) Biology of Anaerobic Microorganisms. John Wiley, New York, pp 469–585
96. Wieland A, Kühl M (2000) Irradiance and temperature regulation of oxygenic photosynthesis and O_2 consumption in a hypersaline cyanobacterial mat (Solar Lake, Egypt). Mar Biol 137:71–85
97. Wieland A, Kühl M (2000) Short-term temperature effects on oxygen and sulfide cycling in a hypersaline cyanobacterial mat (Solar Lake, Egypt). Mar Ecol Prog Ser 196:87–102
98. Wieringa EBA, Overmann J, Cypionka H (2000) Detection of abundant sulphate-reducing bacteria in marine oxic sediment layers by a combined cultivation and molecular approach. Environ Microbiol 2:417–427